Distribution Agreement

In presenting this thesis as a partial fulfillment of the requirements for a degree from Emory University, I hereby grant to Emory University and its agents the non-exclusive license to archive, make accessible, and display my thesis in whole or in part in all forms of media, now or hereafter now, including display on the World Wide Web. I understand that I may select some access restrictions as part of the online submission of this thesis. I retain all ownership rights to the copyright of the thesis. I also retain the right to use in future works (such as articles or books) all or part of this thesis.

Joshua A. Manuel April 12, 2022

A theoretical and experimental study of the population dynamics of abortive infection

by

Joshua A. Manuel

Bruce Levin, Ph.D.
Adviser

Biology

Bruce Levin, Ph.D.
Adviser

Nic Vega, Ph.D.
Committee Member

Katia Koelle, Ph.D.
Committee Member

2022

A theoretical and experimental study of the population dynamics of abortive infection

By

Joshua A. Manuel

Bruce Levin, Ph.D.
Adviser

An abstract of
a thesis submitted to the Faculty of Emory College of Arts and Sciences
of Emory University in partial fulfillment
of the requirements of the degree of
Bachelor of Science with Honors

Biology

2022

Abstract
A theoretical and experimental study of the population dynamics of abortive infection
By Joshua A. Manuel

Bacteria have evolved a number of defenses to protect individual cells and populations from infection by bacteriophage (phage). One such defense is abortive infection (abi), a programmed cell death (suicide) which occurs when a bacterium is infected by a lytic (virulent) phage. Using a mathematical-computer simulations model, I explore the *a priori* conditions under which abi can protect and bacterial populations from infections with lytic phage. To estimate the parameters and test the validity of the predictions of this model, I perform experiments with two abi systems, the Ec48 retron in *Escherichia coli,* and the *abiZ* system in *Lactococcus lactis*. While the results of these experiments are consistent with the predictions of the model, they also suggest that abortive infection is only one step in the defense of these bacteria against phage infection. Within short order of the exposure of these bacteria to phage, envelope resistant mutants emerge and ascend to be the dominant population of bacteria.

A theoretical and experimental study of the population dynamics of abortive infection

By

Joshua A. Manuel

Bruce Levin, Ph.D.
Adviser

A thesis submitted to the Faculty of Emory College of Arts and Sciences
of Emory University in partial fulfillment
of the requirements of the degree of
Bachelor of Science with Honors

Biology

2022

Acknowledgements

I would first like to thank my collaborators whose bacteria strains, plasmids and phage made this study possible. Dr. Rotem Sorek of the Weizmann Institute for the Ec48 bearing *E. coli*. Dr. Frank Oechslin and the Sylvain Moineau Lab of Université Laval for *L. lactis* IL6288 and P335. Dr. Rodolphe Barrangou of North Carolina State University for plasmid pTRK914. Thank you to my committee members Dr. Nic Vega and Dr. Katia Koelle for their feedback and guidance on this project. Thank you to Levin Lab members Kylie Burke, Eduardo Roman, Mason Harvill, Jack Peng, David Goldberg, Jake Fontaine and the late Tom O'Rourke for their constant help and support. Thank you to Brandon Berryhill and Dr. Rodrigo Garcia for their recommendations and guidance on this project. Finally, thank you to Dr. Bruce Levin for serving as my mentor and adviser.

This work was sponsored by MIRA Grant R35 GM 136407 from the US National Institute of General Medical Sciences (BRL).

Table of Contents

A theoretical and experimental study of the population dynamics of abortive infection

Joshua A. Manuel

Introduction

Under the constant threat of phages, bacteria have evolved a number of defenses to prevent lytic (virulent) phage from infecting individual bacteria and protecting bacterial populations from extinction by these phages. The best known and most studied of these mechanisms is envelope resistance, mutations of single genes that modify the receptors to which the phage adsorb and making the bacteria refractory to that phage [1]. In this study, I consider a less well-known defense. Abortive infection (abi) is a programmed cell death (suicide) which occurs when a bacterium is infected by a lytic bacteriophage [2]. Unlike envelope resistance, restriction-modification [3] or CRISPR-Cas [4] abortive infection is not to the advantage of the individual cells expressing this defense but is presumed to evolve by protecting the uninfected clonal cells from infection [5-8].

The genetic basis of abortive infection and mechanisms by which abi kills the infected bacteria and aborts phage infections have been well studied, particularly for the abi systems of *Lactococcus lactis* [9-11] and most recently for an abortive infection system in *Escherichia coli* [12]. On the other hand, relatively little consideration has been given to the long-term population dynamics of lytic phage and bacteria with abortive infection systems. In this study, I use a mathematical–computer simulation model and experiments with the retron Ec48 abortive infection system in *E. coli* and the phage λ^{VIR} and the *abiZ* system in *L. lactis* and the phage P355 to explore the population dynamics of abortive infection.

The Abortive Infection Systems

Retrons, DNA sequences that code for a reverse transcriptase and a unique single-stranded DNA/RNA hybrid called multicopy single-stranded DNA (msDNA), were discovered in 1984 [13] and were the first example of a reverse transcriptase coded for by bacteria [14, 15]. These elements were initially found in *Myxococcus xanthus,* but subsequently have been found in a number of bacterial species, including *Escherichia coli* [16, 17]. Like CRISPR-Cas, retrons are being employed for genome engineering [16-18], and are capable of doing editing tasks that cannot be done by CRISPR-Cas [19]. Also like CRISPR-Cas the function of retrons was not determined for decades after their discovery and molecular characterization [20]. For retrons, the identification of function came in 2020 when Millman and collaborators presented compelling evidence that retrons can defend *E. coli* from infections with lytic phages [12].

The retron studied here is that considered in [12] Ec48 which guards RecBCD, a protein complex which can degrade linear double stranded DNA, such as the DNA phage insert as the first step of the infection cycle [21]. To combat RecBCD, the phage releases RecBCD inhibitors which Ec48 senses and activates a transmembrane effector protein that triggers growth arrest and increased membrane permeability [12]. While Ec48 aborts infections with different phages, for this study I use the phage that in the study by Millman and collegues, seemed most susceptible to abi Ec48, a virulent mutant of lambda, λ^{VIR}. The other system, *abiZ,* is is one of 23 known abortive infection genes in the gram-positive *Lactococcus lactis* [2, 22, 23]. Protection by AbiZ is attributed to its role in premature cell membrane potential collapse and holin precipitation which increases membrane permeability [9]. Although having different mechanistic pathways, both the retron

and AbiZ cause increased cell membrane permeability leading to the early lysis of infected cells preventing phage replication.

Using a mathematical model, I make prediction on the abi bacteria and phage population dynamics in mass, liquid culture. To estimate model parameters and test the validity of these predictions, I use *E. coli* K12 bearing the retron Ec48 described by Millman and colleagues [12] with λ^{VIR}, and *L. lactis* IL6288, a prophage-free strain containing *abiZ* and lytic phage, P335 obtained from the Felix d'Herelle Reference Center for Bacterial Viruses, QC, Canada. Our experiments support the notion that Ec48 and *abiZ* provide protection to their respective population from phages in some capacity. Our models and experiments also indicate that the abortive infection system must induce cell death in nearly all cases to provide this protection on its own. As anticipated by the model, Ec48 reduces or completely eliminates the λ^{VIR} population suggesting high effectiveness of the abi system. *abiZ*, although limiting phage replication and cell death in the short term, allows for the accension of P335 population density. This increase in phage density indicates limited effectiveness of *abiZ* against P335. Despite varying effectiveness of the two systems, in both populations following 24 hours, bacteria with abi develop envelope resistance which can account for the survival of a portion of the populations.

A Model of Abortive Infection

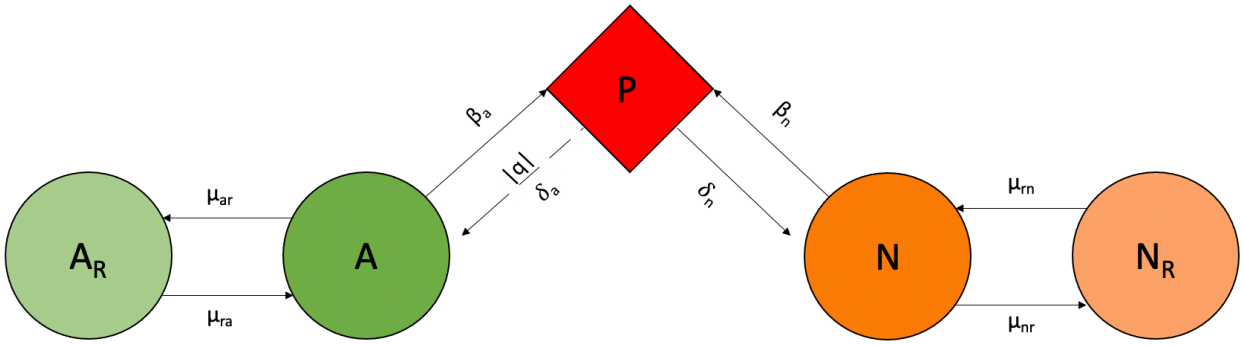

Figure 1. A mass-action diagram representing five populations: a lytic phage (P), a phage-sensitive abi$^+$ bacteria poulation (A), a phage resistant abi$^+$ bacteria population (A_R) a phage-sensitive abi$^-$ bacteria population (N), and a phage-resistant abi$^-$ bacteria population (N_R).

$$\Psi(R) = \frac{R}{R + K}$$

Equation 1

$$\frac{dR}{dt} = -\Psi(R) \cdot e \cdot (v_n \cdot N + v_{nr} \cdot N_r + v_a \cdot A + v_{ar} \cdot A_r)$$

Equation 2

$$\frac{dN}{dt} = \Psi(\mathrm{R}) \cdot (v_n \cdot N - \delta_n \cdot N \cdot P + (\mu_{rn} \cdot N_r - \mu_{nr} \cdot N))$$

Equation 3

$$\frac{dN_r}{dt} = \Psi(\mathrm{R}) \cdot (v_{nr} \cdot N_r - (\mu_{rn} \cdot N_r - \mu_{nr} \cdot N))$$

Equation 4

$$\frac{dA}{dt} = \Psi(\mathrm{R}) \cdot (v_a \cdot A - \delta_a \cdot A \cdot P + (\mu_{ra} \cdot A_r - \mu_{ar} \cdot A))$$

Equation 5

$$\frac{dA_r}{dt} = \Psi(\mathrm{R}) \cdot (v_{ar} \cdot A_r - (\mu_{ra} \cdot A_r - \mu_{ar} \cdot A))$$

Equation 6

$$\frac{dP}{dt} = \Psi(\mathrm{R}) \cdot (\delta_n \cdot \beta_n \cdot P \cdot N - \delta_a \cdot P \cdot q \cdot A + (1 - q) \cdot \delta_a \cdot P \cdot A \cdot \beta_a$$

Equation 7

Figure 2. Differential equations for simulations of abortive infection population dynamics

Parameter	*E. coli* Value (dimensions)	*L. lactis* Value (dimensions)	Description	Source
v_n, v_a, v_{nr}, v_{ar}	2.00(h^{-1})	1.00(h^{-1})	Maximum Growth Rate	Table 2
$\mu_{nr}, \mu_{rn,}$	$1e^{-5}$(per cell per hour)	$3.48e^{-7}$(per cell per hour)	Transitions *N* to N_r and N_r to *N*	[24], Figure S2
μ_{ar}, μ_{ra}	$1e^{-5}$(per cell per hour)	$3.48e^{-7}$(per cell per hour)	Transitions A to A_r and A_r to A	[24], Figure S2
δ_n, δ_a	$2e^{-7}$(ml per cell)	$2.46e^{-7}$(ml per cell)	Adsorption Rate	[24], Figure 7A
β_n, β_a	60 (PFU·CFU^{-1})	17 (PFU·CFU^{-1})	Burst Size	[24], Figure S3
e	$5e^{-7}$(µg per cell)	$5e^{-7}$(µg per cell)	Conversion Efficiency	[25]
K	1	1	Monod Constant	[25]
q	$0 \leq q \leq 1$	$0 \leq q \leq 1$	Effectiveness of abi system	Figure S1

Table 1. Model parameters for simulations of *E. coli*, *L. lactis* and phage population dynamics.

In Figure 1, I illustrate my model of the population dynamics of lytic phage and bacteria with and without an abortive infection system and envelope resistance. There is a single population of phage, P, particles per ml and four bacterial populations of bacteria, A, A_r, N, and N_r cells per ml. The phage sensitive population lacking abi is N. The phage sensitive abi population, A, has a functional abi system. When a phage infects a bacterium of state A, there is a probability q, ($0 \leq q \leq 1$), that the bacteria will die, and the infecting phage will be lost. N_R and A_R, are refractory to the phage and do not allow adsorption of the phage. The N population and 1-q of the A population solely support the replication of the phage.

The bacteria grow at maximum rates, v_a, v_{ar}, v_n, and v_{nr}, per cell per hour, for A, A_r, N and N_r, respectively with the net rate of growth being equal to the product of maximum growth rate, v_{max} and the concentration of a limiting resource, r μg/ml, $v_{max}*\psi(R)$ [26], Equation 1 (Figure 2). The parameter k, the Monod constant, is the concentration of the resource, at which the net growth rate of the bacteria is half its maximum value. By mutation or other processes, the bacteria change states, A→A_r and A_r→A, at rates μ_{er} and μ_{re}, per cell per hour, and N→N_r and N_r→N at rates μ_{nr} and μ_{rn}.

The limiting resource is consumed at a rate equal to the product of $\psi(R)$, a conversion efficiency parameter, e μg/cell [27] and the sum of products of the maximum growth rates of the bacteria and their densities. I assume phage infection is a mass action process that occurs at a rate equal to the product of the density of bacteria and phage and a rate constants of phage infection, δ_e and δ_n (ml/cell) for infections of A and N, respectively [28]. Infections of N by P produce β_n phage

particles, and the (1-q) of the infections of A by P that do not abort, produce β_e phage particles. To account for the decline in physiological state as the bacteria approach stationary phase, R=0, I assume phage infection and mutation rates decline at a rate proportional to Equation 1 (Figure 2). The lag before the start of bacterial growth and latent period of phage infection are not considered in this model or the numerical solution employed to analyze its properties.

The changes in the densities of bacteria and phage in this model are expressed as the series of coupled differential equations (Figure 2).

Computer Simulations of Abortive Infection Protection Against Phage Infection

A.

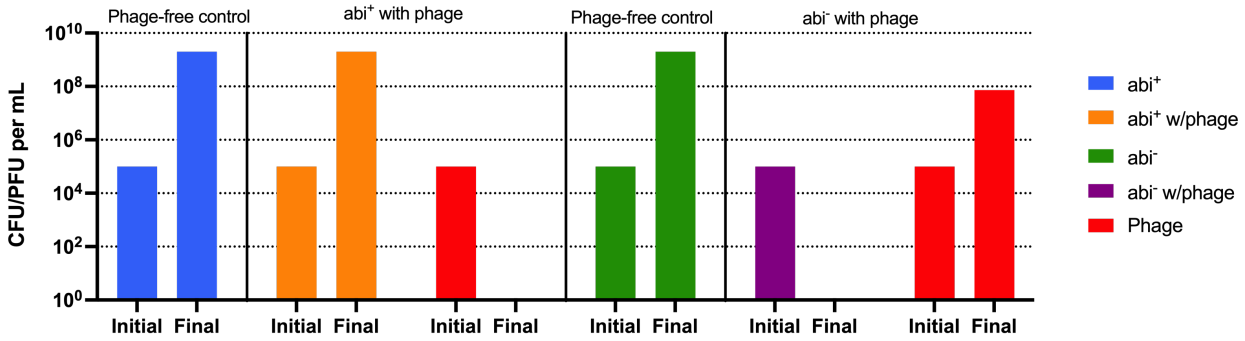

B.

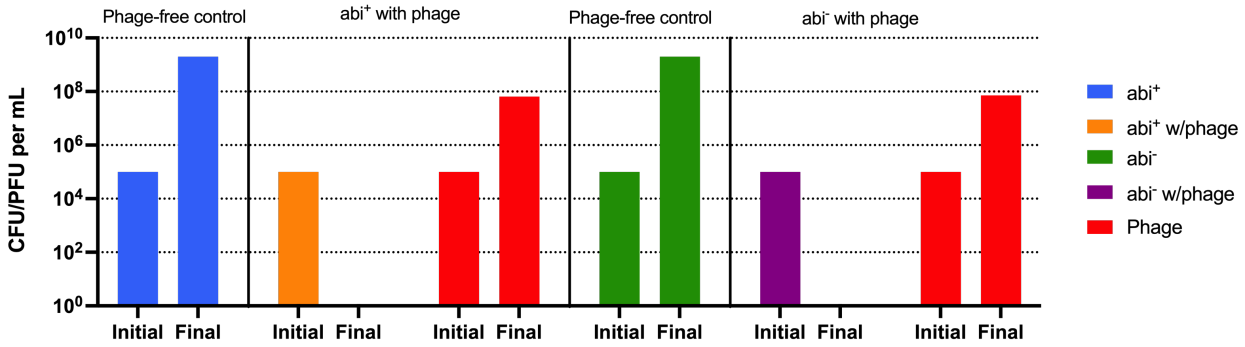

Figure 3. Computer simulation results without envelope resistance. Changes in the densities of an abi^+ bacterial population in the absence (blue) and presence (orange) of phage (red) and an abi^- bacterial population in the absence (green) and presence (purple) of phage at 0 (Initial) and 24 hours (Final). Graphs use *E. coli* parameters: k=1, e= 5×10^{-7} μg/cell, $v_a = v_n = 2.0\ h^{-1}$, $\delta_a=\delta_n=2\times10^{-7}\ h^{-1}cell^{-1}$, $\beta_a=\beta_n=60$ phages/cell, $\mu_{nr}=\mu_{rn}=\mu_{ar}=\mu_{ra}=0$ (not allowing for resistance generation) but are representative of models for *L. lactis*. **A-** A completely effective (q=1.00) abi positive (abi^+) bacterial population in the absence and presence of phage. **B-** An incompletely effective (q=0.95) abi positive (abi^+) bacterial population in the absence and presence of phage.

The consideration of the ability of abortive infection to protect bacterial populations from phage begins with computer simulations showing initial, time 0 hours, and final, time 24 hours, densities of abi^+ and abi^- bacteria in the absence or presence of phage. An analysis was performed to determine the minimum effectiveness of abi to protect a clonal population (q of 0.1 to 1.0, with steps of .01). This analysis determined that abi must abort a minimum of 98% of infections for the retron and 94% for *abiZ* to protect the population from phage (Figure S1). This q value threshold being lower for abiZ is likely explained by the low burst size of P335 (Table 1).

To account for the potential of a partially ineffective abi system, I present a q value of 1.00 and 0.95 in Figures 3A and 3B, respectively, to reflect two systems which are capable and incapable of protection using my *E. coli* parameters as a model (Table 1). As seen in Figure 3A, a completely effective (q=1.00) abi system is able to protect the abi^+ population from the phage. Following 24 hours, the population of abi^+ cells reach their resource limited maximum density and the phage population is lost. However, in Figure 3B, when the abi system is only 95% effective, the abi^+ population is lost, and the phage ascend. The abi^- population is completely lost

when confronted by phage, and the phage reaches its maximum density, limited by host availability.

Population Dynamics of Abortive Infection Systems in Liquid Culture

A.

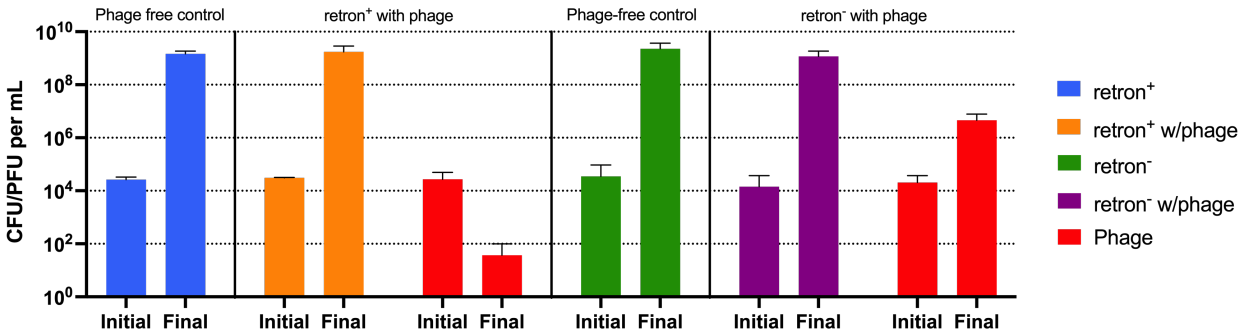

B.

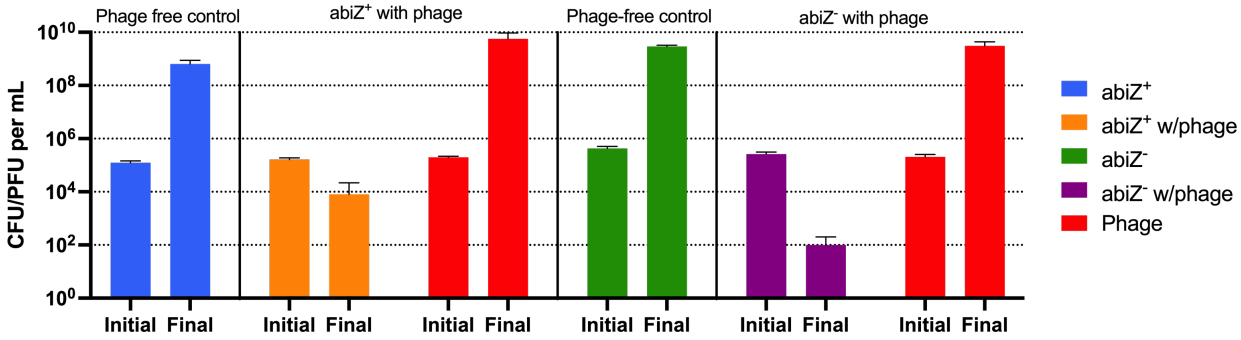

Figure 4. Experimental results of changes in the densities of bacteria and phage at 0 (Initial) and 24 (Final) hours. abi$^+$ bacteria in the absence of phage (blue) and in the presence of phage (orange), an abi$^-$ population of bacteria in the absence (green) of phage (red) and in the presence (purple) of phage. Plotted are the means and standard deviation of the phage and bacterial densities of three independent replicas. **A-** Retron$^+$ and retron$^-$ populations in the absence and presence of the lytic phage λ^{VIR}. **B-** abiZ$^+$ and abiZ$^-$ populations in the absence and presence of P335.

Figure 4A presents the results of the experimental tests of the hypotheses generated by the computer simulations (Figure 3) using the retron mediated abortive infection system Ec48 in *E.*

coli and its lytic phage λ^{VIR}. A retron$^-$ bacteria sensitive to λ^{VIR} was used as a control. As anticipated by the model (Figure 3A), the retron$^+$ population grows to its maximum resource limited density and decreases the density of λ^{VIR}. This decrease in phage can likely be attributed to the retron's low efficiency of plaquing (EOP) of 0 (Figure 5). However, unlike Figure 3A, the control retron$^-$ population and phage both increase in density. A potential explanation for this result would be the evolution of envelope resistance. To test this hypothesis the cross-streak method was used on retron$^-$ colonies isolated after 24 hours to determine susceptibility to λ^{VIR}. By the absence of lytic activity over the isolated colonies, it was determined that envelope resistant retron$^-$ population did emerge after 24 hours. The cross-streak technique was also employed on retron$^+$ colonies following 24 hours and an envelope resistant population was also identified (Table S1)

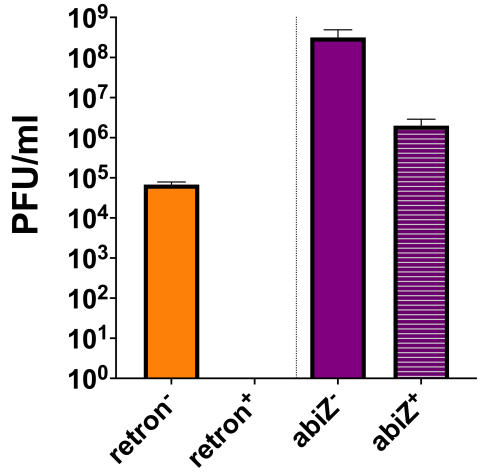

Abi System	EOP ± SD
Ec48 (retron)	0 ± 0.00
abiZ	$6.32e^{-3} \pm 1.02e^{-2}$

Figure 5. Efficiency of Plaquing (EOP) of Ec48 retron and abiZ. Plotted are averages of 6 replicates and error bars represent 1 SD. X axis represents cell type plated on. EOP measured by dividing the number of plaques on abi$^+$ lawn by abi$^-$.

Figure 4B presents the experimental results of *abiZ* in *L. lactis*. As anticipated by Figure 3B and the observed high EOP of *abiZ* (Figure 5) which suggests relatively low effectiveness against P335, the density of $abiZ^+$ decreases and allows for growth of the phage. The $abiZ^-$ population also behaves as expected with the bacteria density decreasing and phage increasing. Although unlike Figure 3B, both $abiZ^+$ and $abiZ^-$ have a small surviving population. Representative colonies of both populations were picked and tested for a change in plaquing efficiency. These results revealed a decrease in P335 plaquing efficiency on the $abiZ^+$ and $abiZ^-$ leading to the conclusion that envelope resistance evolved in *L. lactis* as well (Figure S4).

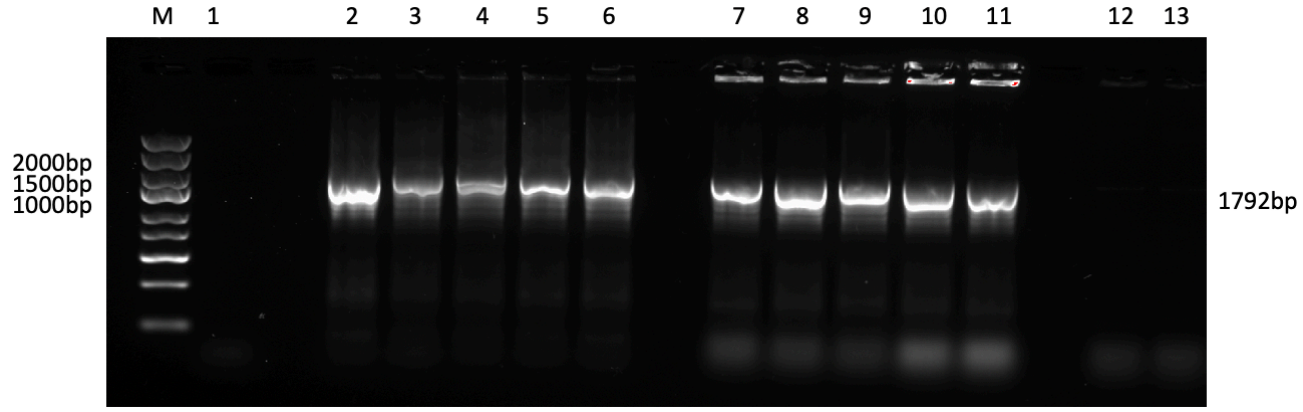

Figure 6. Verification of plasmid pTRK914(pTRK686:*abiZ*) insertion in *L. lactis* IL6288. M: DNA Ladder, 1: Water, 2-6: pTRK914, 7-11: $abiZ^+$, 12-13: $abiZ^-$.

Short Term Dynamics of AbiZ

A.

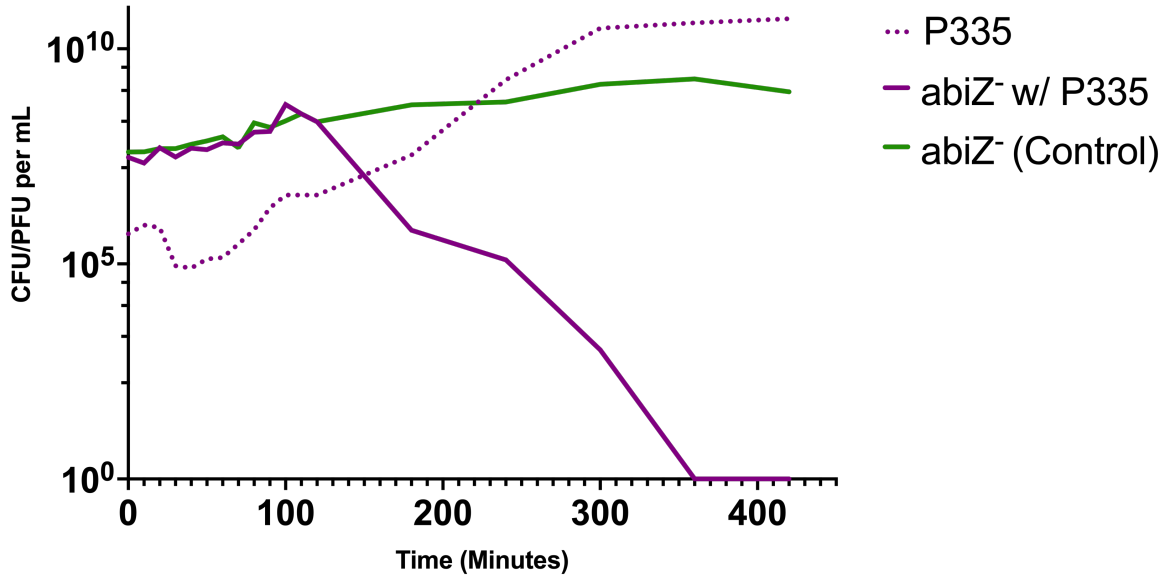

B.

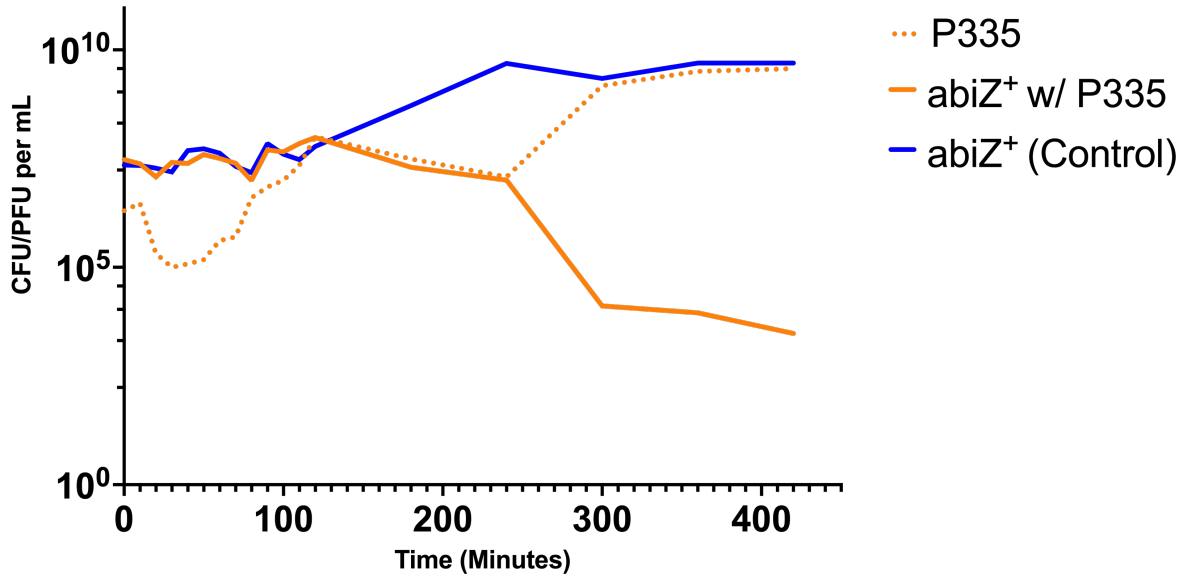

Figure 7. Short term impact of abiZ on densities of bacteria and phage. **A-** abiZ^{-} populations in the absence (green) and presence (purple) of P335 (purple-dashed). **B-** abiZ^{+} populations in the absence (blue) and presence (orange) of P335 (orange-dashed).

To analyze the ability of AbiZ to protect against phage infection in the short term, the densities of phage and bacteria were measured over the first 7 hours of infection (Figure 7). As anticipated, the *abiZ*$^{-}$ population was unable to protect itself from the phage without envelope resitance having evolved. When confronted with P335, the abiZ^{-} population fell below the limit of detection of 10^{1} within 360 minutes and the phage density increased during that time frame (Figure 7A, purple dashed). The *abiZ*$^{+}$ population, however, although still decreasing over a 360 minute interval, did not fall below the limit of detection and slows phage ascension. The P335 population infecting *abiZ*$^{-}$ reached a density >10^{9} PFU/ml in 240 minutes, whereas the phage infecting the *abiZ*$^{+}$ population did not reach the same density until 300 minutes (Figure 7B, orange-dashed). Notably, as seen in the long term experiments (Figure 4B), P335 was still capable of replicating on *abiZ*$^{+}$ cells and reaching a density comparable to the phage replicating on cells lacking the abi system. This is once again likely explained by the high EOP of P335 on *abiZ*$^{+}$ cells.

Computer Simulations of Abortive Infection Accounting for Envelope Resistance and Abi Effectiveness

A.

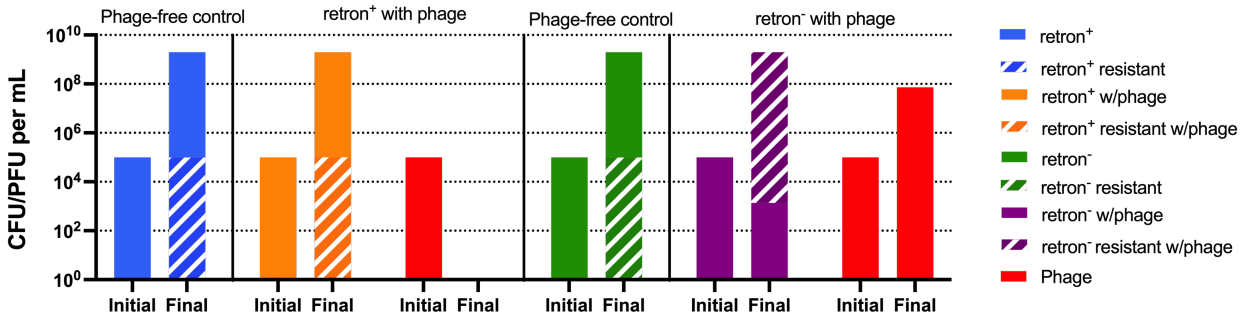

B.

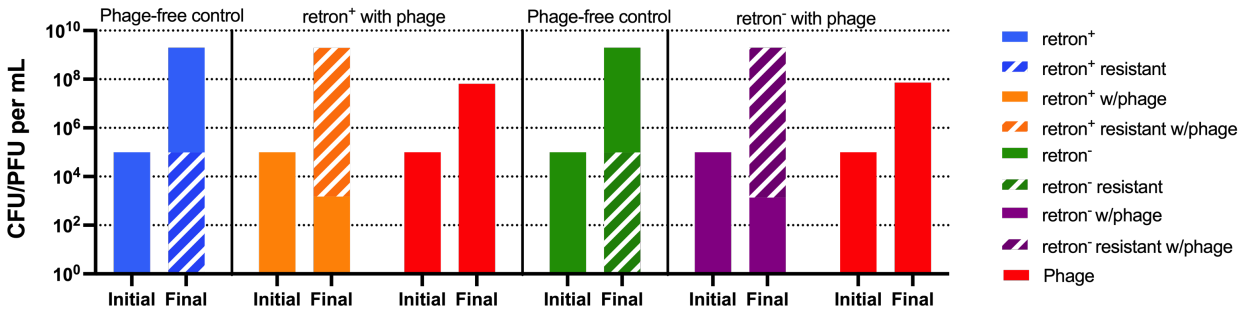

Figure 8. Computer simulations with envelope resistance for *E. coli*. The simulation conditions used are from Table 1. Changes in the densities of a retron$^+$ bacterial population in the absence (blue) and presence (orange) of phage (red) and a retron$^-$ bacterial population in the absence (green) and presence (purple) of phage at 0 (Initial) and 24 hours (Final). The densities of phage resistant mutants are noted by bars with white hashing over the same bar of the sensitive population. **A-** Simulations with a completely effective retron-mediated abi system (q=1.00). **B-** Simulations with a less-than completely effective retron-mediated abi system (q=0.95).

With the addition of a mutation rate in between phage resistant and phage sensitive, μ_{er}, μ_{re}, μ_{nr}, μ_{rn} all being 10^{-5} per cell per hour [24], the model results for the retron very closely resemble the experimental results after 24 hours (Figure 4A) when the retron is completely effective (q=1.00) (Figure 8A). The retron$^+$ population eliminated the phage and the retron$^-$ population grew while still allowing phage growth. For both the retron$^+$ and retron$^-$ populations, envelope resistant cells emerge and are maintained after 24 hours. If the retron were less than 98% effective (Figure 8B), it would be expected the phage population infecting retron$^+$ cells would grow which was not observed in Figure 4A.

Using parameters for *L. lactis*, abiZ and P335, the modeling results (Figure 9) are nearly identical to those of *E. coli* (Figure 8). However, because the *abiZ*$^+$ population allowed for phage growth *in vitro*, the model results when AbiZ is not effective enough to control phage infection

on its own (Figure 9B), q=0.90, more closely resemble the experimental results (Figure 4B). The *abiZ*$^{+}$ population develops envelope resistance, but the phage population grows with both defenses present. My model predicts the resistant population in both *abiZ*$^{+}$ and *abiZ*$^{-}$ to grow to densities much higher than those observed experimentally in Figure 4B. Because the envelope resistant mutants were shown to grow at the same rate as their non-resistant counterparts (Table 2), another mechanism not accounted for by the model must be at play.

A

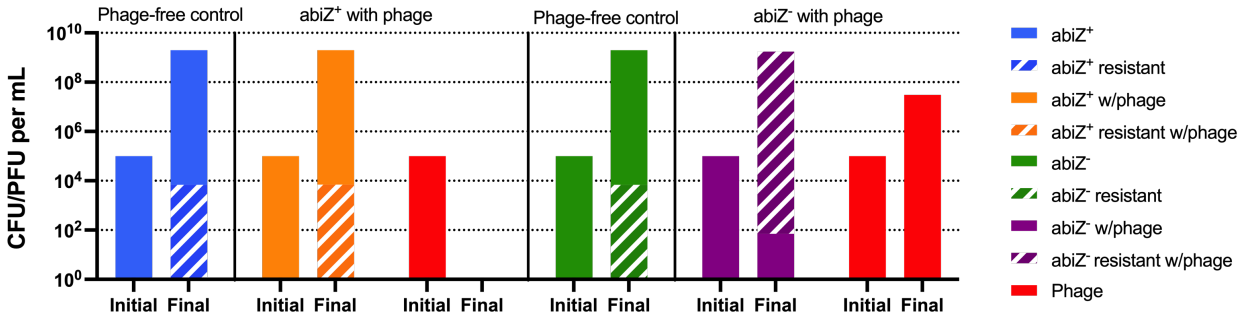

B.

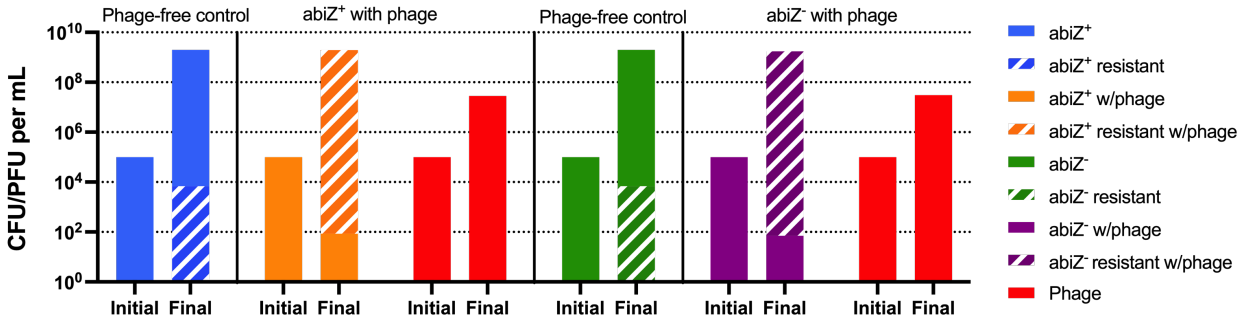

Figure 9. Computer simulations with envelope resistance for *L. lactis*. The simulation conditions used are from Table 1. Changes in the densities of an abiZ^{+} bacterial population in the absence (blue) and presence (orange) of phage (red) and an abiZ^{-} bacterial population in the absence (green) and presence (purple) of phage at 0 (Initial) and 24 hours (Final). The densities of phage resistant mutants are noted by bars with white hashing over the same bar of the sensitive population. **A-** Simulations with a completely effective retron-mediated abi system (q=1.00). **B-** Simulations with a less-than completely effective retron-mediated abi system (q=0.90).

Strain (Population)	Symbol	Growth Rate (h^{-1}) ± SE
E. coli retron$^+$ (A)	v_a	2.27 ± 0.06
E. coli retron$^+$ resistant (A_r)	v_{ar}	2.17 ± 0.02
E. coli retron$^-$ (N)	v_n	2.37 ± 0.04
E. coli retron$^-$ resistant (N_r)	v_{nr}	2.27 ± 0.02
L. lactis abiZ$^+$ (A)	v_a	0.97 ± 0.05
L. lactis abiZ$^+$ resistant (A_r)	v_{ar}	1.04 ± 0.06
L. lactis abiZ$^-$ (N)	v_n	1.06 ± 0.02
L. lactis abiZ$^-$ resistant (N_r)	v_{nr}	1.02 ± 0.07

Table 2. Average growth rates ± one standard error of the mean of 5 replicas of abi$^+$ and abi$^-$ *E. coli* and *L. lactis* with and without envelope resistance.

Discussion

The results of this study provide evidence that two different species of bacteria, gram-negative *E. coli* and gram-positive *L. lactis*, with two different abortive infection systems, Ec48 and *abiZ*, are able to protect themselves from phage infection despite varying abi efficacies. The original model predicted that without the evolution of envelope resistance, bacteria would require a nearly completely effective abi system for survival. This nearly perfect system ($q > 0.98$) was observed in the retron$^+$ population, with an EOP of 0 and reduction in phage density following 24 hours. This model also predicted a relatively ineffective abi system would not provide enough protection for bacteria survival and would allow for phage growth. This result held true for the *abiZ*$^+$ population experimentally as well, with a higher EOP of 6.32×10^{-3}. Although limiting

P335 growth in the short term, the phage was able to grow and reduce bacteria density after 24 hours.

Notably, however, the *abiZ*$^{+}$ cells and retron^{-} cells were not completely eliminated by their respective phages as the model predicted. After testing individuals from these cultures, it was found these populations, as well as the retron^{+} and *abiZ*$^{-}$ populations confronted with phage evolved envelope resistance. This newly evolved phage defense mechanism allowed for the asscent of a phage resistant population regardless of being abi^{+} or abi^{-} in both species of bacteria.

By adding envelope resistance to the model, a more accurate reflection of the experimental observations results. Populations lacking an abortive infection system are able to survive and grow in the presence of phage, perfect abortive infection systems grow and reduce phage density and imperfect systems maintain but allow for phage growth. In all populations confronted by phage, envelope resistant mutants emerge.

Although altruism is very familiar to us eukaryotes, evidence pointing to its existence in prokaryotes is a rarity. Nevertheless, abi presents as inherently altruistic, a programmed death to protect the surrounding population. The question still remains, how does this altruistic trait, abortive infection, evolve and become maintained? This study shows the capaility of abortive infection to protect bacteria from phage in liquid but does not address the population dynamics in a structured environment nor the ability of abi cells to invade when rare. Outside the laboratory, bacteria live in structured environments as colonies. Other studies postulate this structured environment promotes the selection for this extreme form of altruism [5, 6]. Considering this

study's discovery of envelope resistance emerging in abi^+ populations, the possibility this other phage defense mechanism is at play remains and can not be discounted.

Materials and Methods

Numerical solutions – computer simulations.

To analyze the properties of this model Berkeley Madonna was used to solve the differential equations (Figure 2). The growth rate and phage infections parameters used for these simulations are those estimated for *E. col*i and λ^{VIR} or *L. lactis and P335*. Copies of this program are available at www.eclf.net.

Growth media and strains

E. coli cultures were grown at 37 °C in MMB broth (LB broth (244620, Difco) supplemented with 0.1 mM $MnCl_2$ and 5 mM $MgCl_2$). The *E. coli* strain containing the Ec48 retron plasmid was obtained from Rotem Sorek. The sensitive *E. coli* used for controls was *E. coli* C marked with streptomycin resistance, and the Ec48 was marked with ampicillin resistance to differentiate in the invasion experiments. The λ^{VIR} phage lysates were prepared from single plaques at 37 °C in LB medium alongside *E. coli* C. Chloroform was added to the lysates and the lysates were centrifuged to remove any remaining bacterial cells and debris. The λ^{VIR} strain used in these experiments was obtained from Sylvain Moineau.

L. lactis cultures were grown at 30 °C in GM17 broth (M17 broth (Nutri-Bact, Quebec, Canada) supplemented with 0.5% glucose) without shaking. The *L. lactis* strain was obtained from the Felix d'Herelle Reference Center for Bacterial Viruses, QC, Canada. The P335 phage lysates

were prepared from single plaques at 30 °C in LB medium alongside *L. lactis* IL6288. Chloroform was added to the lysates and the lysates were centrifuged to remove any remaining bacterial cells and debris. The P335 strain used in these experiments was obtained from the Felix d'Herelle Reference Center for Bacterial Viruses, QC, Canada.

Sequencing

Sanger sequencing was performed by Eurofins (Louisville, Kentucky) to verify λ^{VIR} using primers borRG1Fw and borRG1Rv (Table S2).

P335 was sequenced using long read technology of Oxford Nanopore Technologies. High titer phage solutions were used to extract phage DNA using Invitrogen's PureLink Viral RNA/DNA extraction kit. After extraction, DNA repair and end-prep occurred followed by adapter ligation and clean-up using a combination of NEBNext Companion Module for Oxford Nanopore Technologies Ligation Sequencing and Nanopore's Ligation Sequencing Kit. In a 0.2 mL PCR tube, 27 µL of nuclease-free water, 20 µL of sample, 1 µL of DNA CS, 3.5 µL of NEBNext FFPE DNA Repair Buffer, 2 µL of NEBNext FFPE DNA Repair Mix, 3.5 µL Ultra II End-prep reaction buffer, and 3 µL of Ultra II End-prep enzyme mix. Tubes were then mixed by flicking and placed onto a thermal cycler and incubated at 20°C for 5 minutes and 65° C for 5 minutes. DNA was then transferred to a new 1.5 mL Eppendorf DNA LoBind tube and 60µL of resuspended AMPure XP beads were added and mixed by flicking. The tubes were then placed on mixer for 5 minutes and incubated at room temperature. Samples were then pelleted on a magnet and the supernatant was pipetted off. 200 µL of 70% ethanol with nuclease-free water was used to wash the beads without disturbing the pellet twice and then pipetted off each time. Beads were left to dry for 30 seconds and then removed from the magnetic rack and resuspended

in 61 µL of nuclease-free water and incubated for 2 minutes at room temperature. The beads were then pelleted on the magnet again and the eluate was removed and retained in a clean 1.5 mL DNA LoBind tube. Next, 60 µL of sample, 25 µL of ligation buffer, 10 µL of NEBNext Quick T4 DNA Ligase, and 5 µL adapter mix were added to a tube and flicked to mix. The reaction was incubated for 10 minutes at room temperature. 40 µL of resuspended AMPure XP beads were added to the reaction and the tube was then incubated on a mixer for 5 minutes at room temperature. The tubes were then pelleted on a magnet rack and the supernatant was removed. The beads were washed and resuspended in 250 µL of Long Fragment Buffer, pelleted using the magnet, and the supernatant was removed twice. The samples were then allowed to dry for 30 seconds and then resuspended in 15 µL of Elution Buffer and incubated for 10 minutes at room temperature. Beads were then pelleted, and the eluate was removed and retained in a fresh 1.5 mL DNA LoBind tube. These samples could now be stored in the fridge for up to a week before processing. The SpotON flow cell was then loaded MinION and sample preparation was followed by using the ligation kit and high accuracy base calling with specifications of QScore of at least 7 and reads of at least 20 KB were collected and sequenced for an hour before the process was terminated and the sequences were exported for analysis.

16s rDNA sequence determination was performed by Eurofins (Louisville, Kentucky) to verify *L. lactis* IL6288 and *E. coli* C identities using primers 16S rRNA For and Rev (Table S2).

L. lactis **Plasmid Electroporation and Strain Preparation**

Plasmid pTRK914(pTRK686:abiZ) was kindly shared by Rodolphe Barrangou at NCSU and was electroporated into IL6288 using methods adapted from [29]. Electrocompetent cells were prepared from a culture of IL6288 grown to an OD of 0.2 in 250mL GM17 supplemented with

0.2M sucrose and 1% glycine. Following electroporation, cells were grown in GM17 supplemented with 0.2M sucrose, 20mM MgCl2 and 2mM $CaCl_2$. Cells were plated on GM17 agar (1.1% agar) supplemented with 5ug/ml chloramphenicol to isolate transformants.

PCR and Gel Electrophoresis

pTRK914 incorporation was verified by PCR which was carried out using Thermo Scientific's (Lithuania) Phusion Blood Direct PCR Master Mix (Cat# F-175L) and primers JMP2Fw2 and JMPRv2 built in PrimerBlast (NCBI) to amplify *abiZ* gene (Supp Fig Primer). Products were visualized on a 1% agarose/TAE gel with Biotium's (USA) 10,000X GelRed Nucleic Acid Stain and the O'GeneRuler Express DNA Ladder (Cat# SM1553, Thermo Scientific).

Sampling bacterial and phage densities

E. coli bacteria and phage densities were estimated by serial dilution in 0.85% saline followed by plating. The total density of bacteria was estimated on LB hard (1.6%) agar plates. To estimate the densities of free phage, chloroform was added to suspensions before serial dilution. These suspensions were plated at various dilutions on lawns made up of 0.1 mL of overnight LB-grown cultures of *E. coli* C (about 5×10^8 cells per mL) and 4 mL of LB soft (0.65%) agar on top of hard (1.6%) LB agar plates.

L. lactis bacteria and phage densities were estimated by serial dilution in 0.85% NaCl saline followed by plating. The total density of bacteria was estimated on GM17 hard (1.6%) agar plates. To estimate the densities of free phage, chloroform (J.T. Baker) was added to suspensions before serial dilution. These suspensions were plated at various dilutions on lawns made up of 0.1 mL of overnight GM17-grown cultures of *L. lactis* IL6288 (about 2×10^9 cells per mL) and 4

mL of GM17 soft (0.65%) agar supplemented with 10mM $CaCl_2$ on top of hard (1.6%) GM17 agar plates supplemented with 10mM $CaCl_2$.

Efficiency of Plaquing

Lysate of know phage titer was serially diluted and plated on abi+ (retron+ or abiZ+) or abi- lawn. PFU/ml on abi+ lawn was divided by PFU/ml on abi- lawn to get efficiency of plaquing.

Resistance testing with cross streaks

E. coli were tested by streaking in straight lines ten colonies from 24-hour plates across 20 μL of a λ^{VIR} lysate (>10^8 plaque-forming units [pfu]/mL) on LB hard (1.6%) agar plates. Susceptibility to λ^{VIR} was noted as breaks in the lines of growth. Continuous lines were interpreted as evidence for resistance.

Resistance testing with plaquing efficiency

L. lactis were tested by choosing colonies from liquid culture experiments and growing up in 10mL of GM17 broth for 24 hours. P335 lysate was plated at various dilutions on lawns made up of 0.1mL of these cultures (about 2×10^9 cells per mL) and 4 mL of GM17 soft (0.65%) agar supplemented with 10mM $CaCl_2$ on top of hard (1.6%) GM17 agar plates supplemented with 10mM $CaCl_2$. Efficiency of plaquing was calculated by dividing the PFU/ml of P335 on resistant lawn divided by PFU/ml on non-resistant lawn.

Model Parameter Estimations

E. coli growth rates were estimated in a Bioscreen C. 48-hour overnights of each strain to be tested were diluted in MMB broth to an initial density of approximately 10^5 cells per ml. 10 replicas of each strain were loaded into 100-well plates and grown at 37c with shaking for 24 hours taking OD (600nm) measurements every five minutes.

L. lactis growth rates were estimated in a Bioscreen C. 48-hour overnights of each strain to be tested were diluted in GM17 broth to an initial density of approximately 10^5 cells per ml. 10 replicas of each strain were loaded into 100-well plates and grown at 30°C without shaking for 24 hours taking OD (600nm) measurements every five minutes with shaking before each measurement.

The parameters critical for the interaction of λ^{vir} with *E. coli* and *L. lactis* with P335 used in this study were estimated in independent experiments in LB medium or GM17 respectively. Phage burst sizes (β) were estimated with one-step growth experiments [30] in a manner similar to [31]. Adsorption of λ^{vir} to *E. coli* was estimated as described in [25] and P335 to *L. lactis* using an exponential regression of experimental short term densities.

Short term experiments

Approximately 10^7 CFU/ml *L. lactis* was added to GM17 broth supplemented with 10mM $CaCl_2$ and grown for 1 hour at 30ºC without shaking. Following 1 hour, approximately 10^6 PFU/ml P335 was added. Bacteria and phage were cultured at 30ºC. Bacteria and phage density was measured every 10 minutes for 2 hours and every hour for another 4 hours.

Liquid culture experiments

E. coli overnight cultures grown at 37°C in MMB Broth were serially diluted in 0.85% saline to approximate initial density and 100 µL were added to flasks containing 10 mL MMB. λ^{VIR} lysate (>10^8 pfu/ml) was serially diluted to an MOI of ~1 and 100 µL was added to the appropriate flask. These flasks were sampled for both phage and bacterial initial densities (t = 0 h) and were

then grown at 37°C with constant shaking. The flasks were, once again, sampled for phage and bacterial densities (t = 24 h).

L. lactis overnight cultures grown at 30°C in GM17 Broth were serially diluted in 0.85% saline to approximate initial density and 100 µL were added to culture tubes containing 10 mL GM17 supplemented with 10mM $CaCl_2$. P335 lysate (>10^8 pfu/ml) was serially diluted to an MOI of ~1 and 100 µL was added to the appropriate tube. These tubes were sampled for both phage and bacterial initial densities (t = 0 h) and were then grown at 30°C without shaking. The tubes were, once again, sampled for phage and bacterial densities (t = 24 h).

Supplemental Material

A.

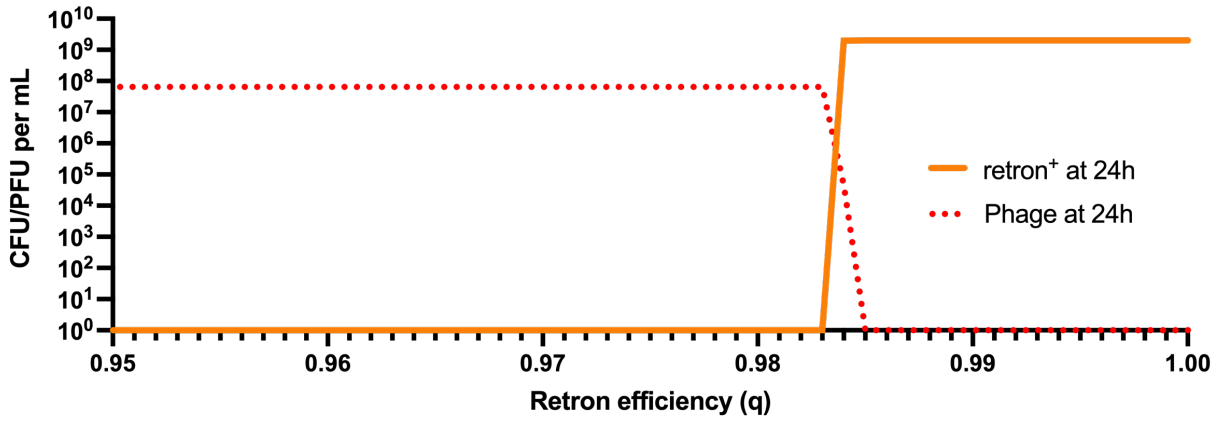

B.

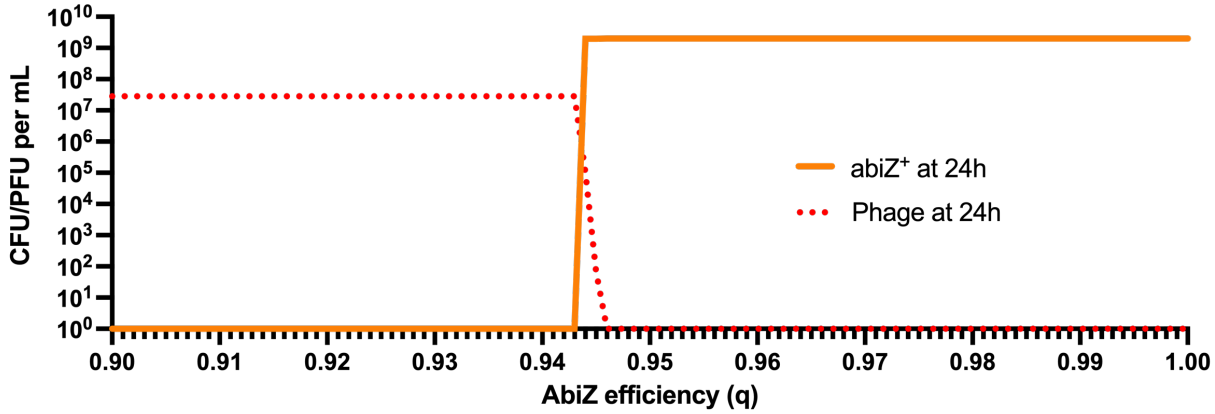

Figure S1. Computer simulation results for the effect of abi efficiency as values of q. Plotted are the 24-hour densities of phage and abi$^+$ bacteria for varying values of q. The parameters used are the same as those in Table 1 without the transition to and from resistant.

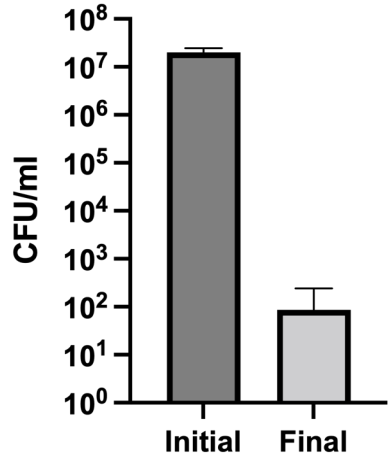

Figure S2. Fluctuation test to measure mutation rate to phage resistant of *L. lactis* IL6288. Initial and average surviving cells CFU/ml after 24 hours (Final) of 10 replicas and standard deviations (error bars) grown with P335.

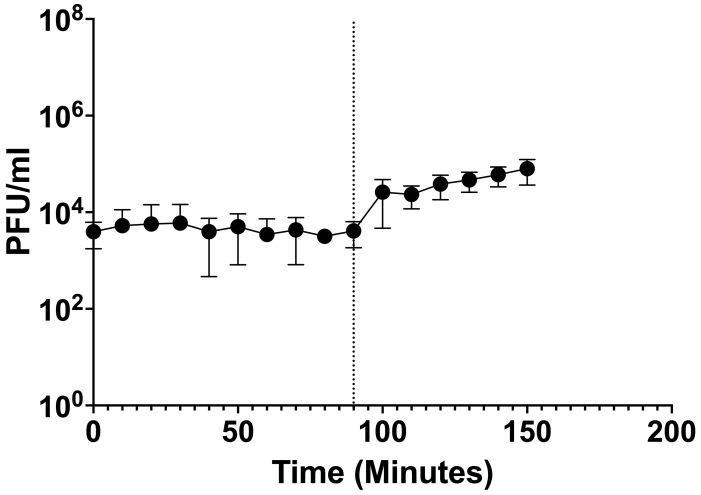

Figure S3. One step growth curve of P335 grown on IL6288. Average PFU/ml ± 1 SD shown with approximate burst time represented by the dotted line

Strain	Plate Number	Resistant Ratio
	1	1
	2	1

E. coli (retron^{+})	3	1
	4	1
	5	1
	6	1
	7	1
	8	1
	9	1
	10	1
E. coli C (retron^{-})	1	1
	2	1
	3	1
	4	.9
	5	1
	6	1
	7	1
	8	1

	9	1
	10	1

Table S1. Cross streak results to test for resistance of *E. coli*. Resistant ratio measured as a number of resistant colonies divided by total number of colonies tested (10) per culture.

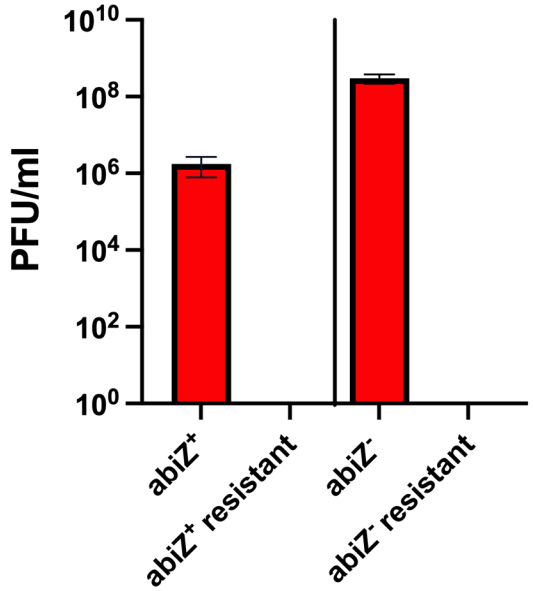

Figure S4. Test for resistance in *L. lactis*. Bars represent average PFU/ml of 4 replicates of P335 on abiZ$^+$, abiZ$^-$ and phage resistant mutants. Error bars represent 1 SD.

Primer Name	Primer Sequence
JMP2Fw	5’ GCT CAA GGG CTT TTA CGC TAC 3’
JMP2Rv	5’ TGT CAC TAA CCT GCC CCG TT 3’
ReadyMade™ Primers (Integrated DNA-Technologies, USA) 16S rRNA For	5’ AGA GTT TGA TCC TGG CTC AG 3’

ReadyMade™ Primers (Integrated DNA-Technologies, USA) 16S rRNA Rev	5’ ACG GCT ACC TTG TTA CGA CTT 3’
borRG1Fw	5’ GCT CTG CGT GAT GAT GTT GC 3’
borRG1Rv	5’ GCA GAG AAG TTC CCC GTC AG 3’

Table S2. Primer name and sequences used in verification of pTRK914 incorporation and strain sequence verification.

References

1. Levin, B.R. and J.J. Bull, *Population and evolutionary dynamics of phage therapy.* Nat Rev Microbiol, 2004. **2**(2): p. 166-73.
2. Labrie, S.J., J.E. Samson, and S. Moineau, *Bacteriophage resistance mechanisms.* Nat Rev Microbiol, 2010. **8**(5): p. 317-27.
3. Korona, R., B. Korona, and B.R. Levin, *Sensitivity of naturally occurring coliphages to type I and type II restriction and modification.* J Gen Microbiol, 1993. **139 Pt 6**: p. 1283-90.
4. Deveau, H., J.E. Garneau, and S. Moineau, *CRISPR/Cas system and its role in phage-bacteria interactions.* Annu Rev Microbiol, 2010. **64**: p. 475-93.
5. Berngruber, T.W., S. Lion, and S. Gandon, *Evolution of suicide as a defence strategy against pathogens in a spatially structured environment.* Ecol Lett, 2013. **16**(4): p. 446-53.
6. Fukuyo, M., A. Sasaki, and I. Kobayashi, *Success of a suicidal defense strategy against infection in a structured habitat.* Sci Rep, 2012. **2**: p. 238.
7. Lopatina, A., N. Tal, and R. Sorek, *Abortive Infection: Bacterial Suicide as an Antiviral Immune Strategy.* Annu Rev Virol, 2020. **7**(1): p. 371-384.
8. Refardt, D., T. Bergmiller, and R. Kummerli, *Altruism can evolve when relatedness is low: evidence from bacteria committing suicide upon phage infection.* Proc Biol Sci, 2013. **280**(1759): p. 20123035.
9. Durmaz, E. and T.R. Klaenhammer, *Abortive phage resistance mechanism AbiZ speeds the lysis clock to cause premature lysis of phage-infected Lactococcus lactis.* J Bacteriol, 2007. **189**(4): p. 1417-25.
10. Emond, E., et al., *AbiQ, an abortive infection mechanism from Lactococcus lactis.* Appl Environ Microbiol, 1998. **64**(12): p. 4748-56.
11. Haaber, J., et al., *AbiV, a novel antiphage abortive infection mechanism on the chromosome of Lactococcus lactis subsp. cremoris MG1363.* Appl Environ Microbiol, 2008. **74**(21): p. 6528-37.
12. Millman, A., et al., *Bacterial Retrons Function In Anti-Phage Defense.* Cell, 2020. **183**(6): p. 1551-1561 e12.

13. Yee, T., et al., *Multicopy single-stranded DNA isolated from a gram-negative bacterium, Myxococcus xanthus.* Cell, 1984. **38**(1): p. 203-9.
14. Inouye, S., et al., *Reverse transcriptase associated with the biosynthesis of the branched RNA-linked msDNA in Myxococcus xanthus.* Cell, 1989. **56**(4): p. 709-17.
15. Temin, H.M., *Reverse transcriptases. Retrons in bacteria.* Nature, 1989. **339**(6222): p. 254-5.
16. Rice, S.A. and B.C. Lampson, *Phylogenetic comparison of retron elements among the myxobacteria: evidence for vertical inheritance.* J Bacteriol, 1995. **177**(1): p. 37-45.
17. Simon, D.M. and S. Zimmerly, *A diversity of uncharacterized reverse transcriptases in bacteria.* Nucleic Acids Res, 2008. **36**(22): p. 7219-29.
18. Rice, S.A., et al., *Diversity of retron elements in a population of rhizobia and other gram-negative bacteria.* J Bacteriol, 1993. **175**(13): p. 4250-4.
19. Brownwell, L., *Move over CRISPR, the retrons are coming.* Wyss Institute Impact Report, 2021.
20. Ishino, Y., et al., *Nucleotide sequence of the iap gene, responsible for alkaline phosphatase isozyme conversion in Escherichia coli, and identification of the gene product.* J Bacteriol, 1987. **169**(12): p. 5429-33.
21. Cheng, K., et al., *A conformational switch in response to Chi converts RecBCD from phage destruction to DNA repair.* Nat Struct Mol Biol, 2020. **27**(1): p. 71-77.
22. Chopin, M.C., A. Chopin, and E. Bidnenko, *Phage abortive infection in lactococci: variations on a theme.* Curr Opin Microbiol, 2005. **8**(4): p. 473-9.
23. Coffey, A. and R.P. Ross, *Bacteriophage-resistance systems in dairy starter strains: molecular analysis to application.* Antonie Van Leeuwenhoek, 2002. **82**(1-4): p. 303-21.
24. Chaudhry, W.N., et al., *Leaky resistance and the conditions for the existence of lytic bacteriophage.* PLoS Biol, 2018. **16**(8): p. e2005971.
25. Levin, B.R., Frank M. Stewart, and Lin Chao., *Resource-limited growth, competition, and predation: a model and experimental studies with bacteria and bacteriophage.* The American Naturalist, 1977. **111**(977): p. 3-24.
26. Monod, J., *The growth of bacterial cultures.* Annual Review of Microbiology, 1949. **3**: p. 371-394.
27. Stewart, F.M. and B.R. Levin, *Resource partitioning and the outcome of interspecific competition: a model and some general considerations.* American Naturalist, 1973. **107**: p. 171-198.
28. Chao, L., B.R. Levin, and F.M. Stewart, *A complex community in a simple habitat: an experimental study with bacteria and phage.* Ecology, 1977. **58**: p. 369-378.
29. Holo, H. and I.F. Nes, *High-Frequency Transformation, by Electroporation, of Lactococcus lactis subsp. cremoris Grown with Glycine in Osmotically Stabilized Media.* Appl Environ Microbiol, 1989. **55**(12): p. 3119-23.
30. Ellis, E.L. and M. Delbruck, *The Growth of Bacteriophage.* J Gen Physiol, 1939. **22**(3): p. 365-84.
31. Abedon, S.T., T.D. Herschler, and D. Stopar, *Bacteriophage latent-period evolution as a response to resource availability.* Appl Environ Microbiol, 2001. **67**(9): p. 4233-41.